

Behavior of gusset plate-T0-CCFT connections with different configurations

M.M. Hassan ^{1a}, H.M. Ramadan ^{*1}, M. Naeem ^{2b} and S.A. Mourad ^{1c}

¹ Faculty of Engineering (Steel Department), Cairo University, Cairo, Egypt

² Faculty of Engineering (Structural Department), Cairo University, Cairo, Egypt

(Received December 13, 2012, Revised March 12, 2014, Accepted April 16, 2014)

Abstract. Concrete-filled steel tube (CFT) composite columns, either circular (CCFT) or rectangular (RCFT), have many economical and aesthetic advantages but the behavior of their connections are complicated. This study aims to investigate, through an experimental program, the performance and behavior of different connections configurations between circular concrete filled steel tube columns (CCFT) and gusset plates subjected to shear and axial compression loadings. The study included seventeen connection subassemblies consisting of a fixed length steel tube and gusset plate connected to the tube end with different details tested under half cyclic loading. A notable effect was observed on the behavior of the connections due to its detailing changes with respect to capacity, failure mode, ductility, and stress distribution.

Keywords: concrete filled tube (CFT) columns; connections; ductility; strength; connection detailing

1. Introduction

Concrete filled steel tube (CFT) columns are widely used in composite steel-concrete braced steel frames due to the gained advantages from combining concrete and steel. They increase the frames stiffness compared to open steel sections and decrease construction costs as they preclude the use of shuttering. The use of braced frames becomes indispensable especially in multi-story buildings to reach the drift limits recommended by the design codes. However, the main drawback of using CFT columns is the complexity of their connections. Although there is a wide range of connections that can be used with composite construction, designers usually face difficulties and insufficient design data when dealing with brace-to-column connections of composite braced frames with (CFT) columns. Additionally, the used design formulas may yield connections that might have capacities dissimilar to what was anticipated. The AISC specifications (2010) allow considering load transfer mechanisms which include direct bearing, shear connection, or direct bond interaction. These mechanisms are allowed to be considered separately due to lack of data on

*Corresponding author, Associate Professor, E-mail: rhazem2003@yahoo.com

^a Assistant Professor

^b Professor

^c Professor

how to combine them as reported by Jacobs and Hajjar (2010).

During earthquake excitation, the brace-to-column connection should ensure that the load is transferred to both steel and concrete in a manner that ensures satisfactory seismic performance of the system. Roeder *et al.* (2004) provided an overview of the seismic demands on the connection of the CFT braced frame systems through an experimental program. Also MacRae *et al.* (2004) performed experimental and numerical study on different configurations of brace-to-column connections in order to evaluate the bearing stress on concrete in partially loaded CFT columns. The studied gusset plate to CCFT column connections parameters were thickness of tube and gusset plate, coefficient of friction between steel and concrete, and the level of axial force. The authors stated that the force was transferred to the composite column by mainly two mechanisms: the bearing under the gusset plate and friction between steel plate and concrete core or steel tube. The percentage of the force carried by the second mechanism is 30% of the total transferred force. However, this part is usually neglected as quantifying the force transferred by friction in actual situations is hard due to the shrinkage of concrete. Moreover, it was observed that the effect of shear studs is negligible in transferring force between steel and concrete. Hajjar *et al.* (2012) and Denavit and Hajjar (2012) performed an experimental program in order to develop rational design recommendations for the design of composite columns. The authors highlighted the lack of guidance regarding the design of composite braced frames. Consequently, experimental testing is needed to fill the gaps within the available data. Moreover, tests on full-scale composite braced frames with CFT columns under pseudo-dynamic loading were conducted in order to give insight to the global behavior of system and the effect of connections as reported by Tsai and Hsiao (2008). Many researchers such as Whitmore (1952), Yam and Cheng (2002), Roeder *et al.* (2004), and Gross (1990) have investigated the behavior of gusset plate connections in braced frames. It was found that the capacity of gusset plate connections is affected by thickness of gusset plate, brace inclination angle, and existence of stiffeners.

Analytical studies were conducted by MacRae *et al.* (2004) and Hu *et al.* (2011) to analyze the behavior of gusset plate CFT-to-bracing connections while considering a wide range of parameters such as the load ratio on the CFT column, thickness of gusset plate, and introduction of cutouts. Generally, failure of the connection was observed under the connection area. It was also found that increasing the thickness of gusset plate or introducing of cutouts has small effect on the ultimate strength of CFT column; yet they would cause more local bulged shapes on the steel tube below the connection area.

The main goal of this paper is to present the full results obtained from an experimental program carried out to investigate behavior and strength of different configurations of gusset plate to CCFT columns connection under the action of compressive cyclic loading between zero and a value increasing till the capacity of the connection. The loads are applied parallel and perpendicular to the columns axis creating shear and compression on the gusset plates. The data extracted from the tests will be used to perform a parametric study to addressing the effect of various parameters. It is also aimed to study the effect of connection detailing on its behavior, load capacity and failure mode which are considered as key aspects for the development of design provisions for such connections as explained through the preliminary analysis of results (Hassan *et al.* 2013).

2. Experimental program

2.1 Specimen details

A series of seventeen tests designed to investigate the behavior, load capacity and failure mode of gusset plate to CCFT connections was carried out to failure in the laboratory of American University in Cairo. The studied parameters were the connection configuration, the direction of

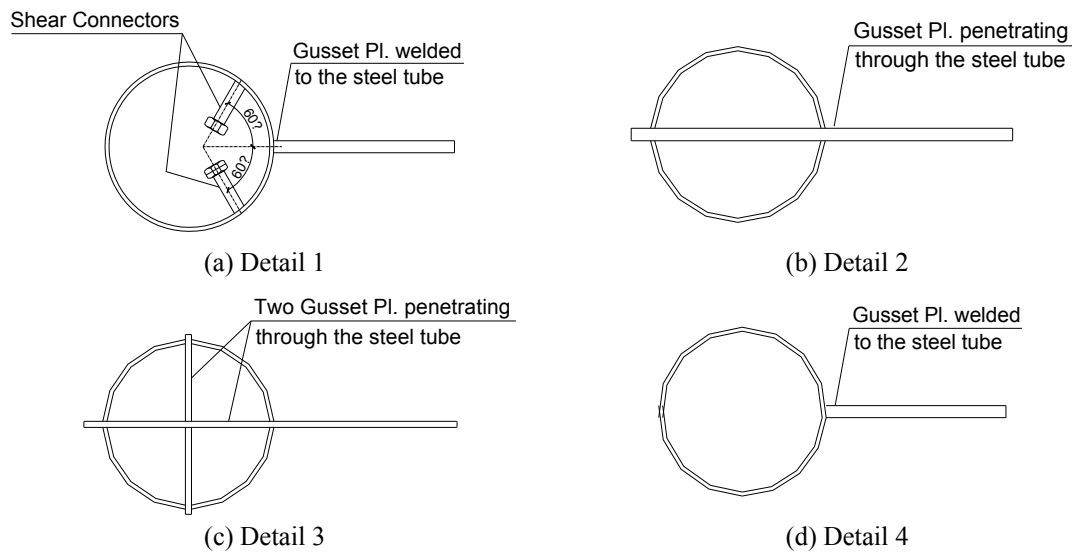


Fig. 1 Configuration of different studied connection details

Table 1 Summary of Tested Subassemblies

Test group	Detail No.	Test unit	D (mm)	t (mm)	t _g (mm)	Concrete infill	Steel mat.	Pipe mat.	F _{cu} MPa	F _{c'} MPa	Loading direction
A	1	SP-H1	168.3		12	Filled			47.2	37.8	Perpendicular [Compression]
	2	SP-H2	168.3	5	12				50.8	40.6	
B	1	H-1			12	Filled			21.2	16.7	Perpendicular [Compression]
	2	H-2			12						
	3	H-3	114.3	3	6						
	4	H-4			12						
	4	H-5			12						
C	1	V-1			12	Filled	A36	A53 Gr-A	21.2	16.7	Parallel [Shear]
	2	V-2			12						
	3	V-3	114.3	3	6						
	4	V-4			12						
	4	V-5			12						
D	1	H-1			12	Filled			26.3	20.7	Perpendicular [Compression]
	2	H-2			12						
	3	H-3	114.3	3	12						
	4	H-4			12						
	4	H-5			12						

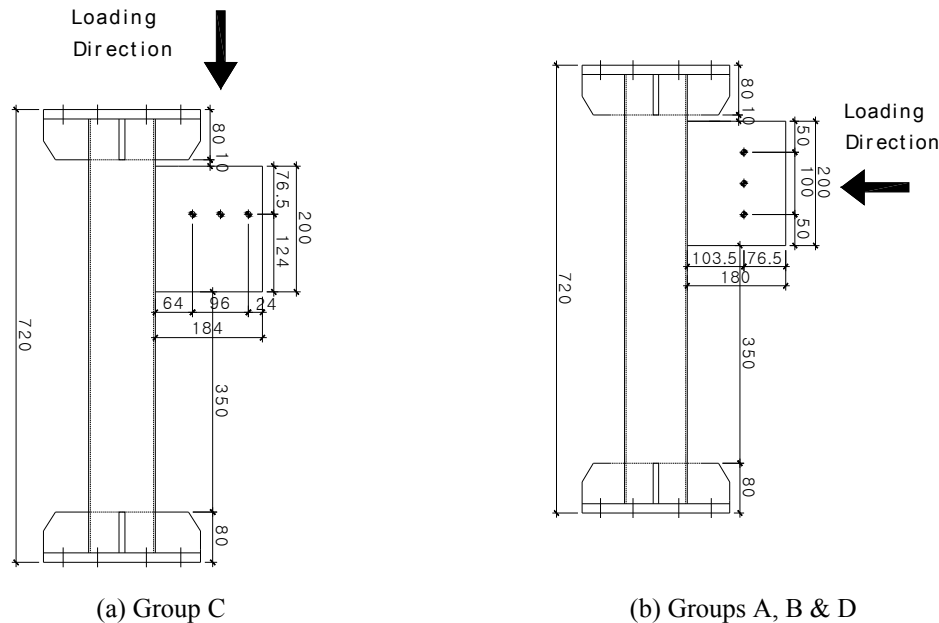


Fig. 2 General dimensions of tested groups Specimens

load application as well as the thickness of gusset plate. All other parameters that may affect the connection behavior such as pipe size, pipe thickness and plate edge distance were fixed. Fig. 1 shows a general layout of the different tested connections which are summarized and listed in Table 1. The tests were divided to three groups A, B, C & D depending on the loading and pipe size used. The connection details were divided into four types' No. 1, 2, 3, and 4. Type 1 refers to connections with gusset plate welded directly to the steel tube shell with provision of shear connectors welded within the connections zone and embedded inside concrete. Type 2 refers to connections with gusset plate fitting within slots in the steel tube. Type 3 refers to connections are similar to type 2 with an additional gusset plate welded perpendicular to the penetrating gusset plate. Finally, type 4 refers to connections with gusset plate is welded directly to the steel tube shell which is considered as pilot connections. The connections with different configurations are attached to the specimens' ends to avoid the effect of its deformation at mid-span on connection behavior. Table 1 also shows the pipe diameter, D , shell thickness, t , and the thickness of the connection gusset plate, t_g , which varies according to the connection details and load application. Part of test specimens after concrete pouring is shown in Fig. 2. The specimens consisted of a small part of circular pipe fabricated from 114 or 168 mm diameter, which represent a part of CFT column, connected to stiffened steel seats by bolting. The length of specimens was fixed to be 680 mm. The distance between the gusset plate edge and all the specimen ends was 90 mm. This distance was chosen as the least probable distance in order to decrease the moment applied on the steel tube to the least value. The dimensions of specimens are shown in Fig. 3. Maximum allowable fillet weld sizes are used to join the gusset plate to the steel tube that performed using E70 electrodes. In order to ensure a ductile behavior at failure of connections, the strength capacity of the connection elements should be higher than the connecting members. This is applied for all tested specimens except for SP-H1 and SP-H2 that they are designed in such a way that the CFT

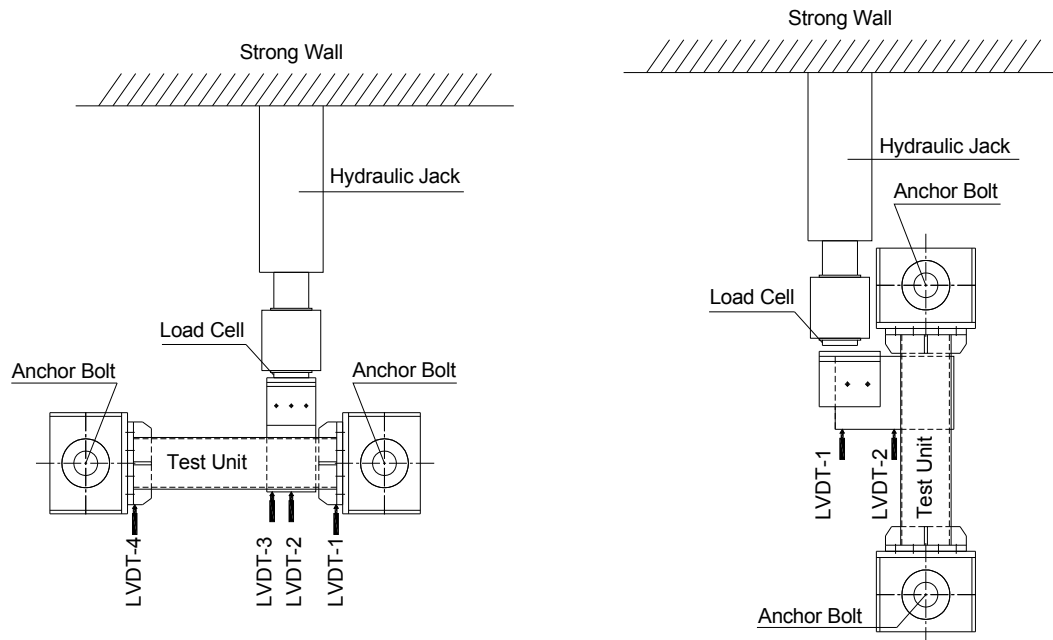


Fig. 3 Plan of test set-up for loaded specimens

was stronger than the connection. Connections with details 2 and 3 are designed in such a way that they have the same bearing area on the concrete. This resulted in using a gusset plate with half of the thickness used in detail 2 connections. This was typically followed in Test groups B and C. However, the gusset plate thickness is fixed in Test group D in order to study the behavior of the connection regardless of the thickness of the gusset plate.

2.2 Test configuration

The basic test setup is composed of the tested specimens, supporting system, and loading system as shown in Fig. 3. The supporting system is designed to be compatible with the lab facilities available such as strong wall, strong floor, and rigid frame. The hydraulic mechanical actuator with capacity 1400 kN and ± 400 mm stroke was supported by the strong wall from one of its sides. It was attached to the specimen from the other side through a thick plate and two angles connected to the end of the connection gusset plate. The compression load is applied on the specimens in two different directions, parallel and perpendicular compression to the specimen axis, to simulate the vertical and horizontal components of the forces that can be applied on the connections. It can be seen that specimens were supported at one central point at each end which resulted in rotating of the whole specimen around these points. Therefore, the additional rotation and displacement are subtracted from the results. Great care was given to leveling of the specimens to ensure that it was correctly aligned during testing.

2.3 Material properties

The tested specimens included steel columns pipes, steel plates, and concrete infill. Five test

coupons were taken from the pipes and gusset plates to evaluate the mechanical properties through tensile tests. Four of them were cut out from the ends of steel pipes that made of A53Gr-A materials and composing the columns after the completion of the experiments and the last was taken from the gusset plates. The principle material properties measured in these tests are reported in Table 2. Connecting angles and gusset plates were made of St 37-2 [A36]. The used shear studs were of grade (8.8) which stands for yield strength and ultimate strength equal to 640 and 800 MPa, respectively. Besides, quality control during the mixing of concrete was made by the determination of mechanical properties of concrete by testing of $150 \times 150 \times 150$ mm standard cubes and 150 mm diameter and 300 mm height standard cylinder. The control specimens are casted in the same time of pouring concrete in columns. The mean compressive strength of concrete cylinders (f_c') after 28 days is equal to 38.0 MPa for test group A and equal to 16.7 MPa for test group B and C. Table 1 shows the concrete compressive strength that was estimated at the testing day.

2.4 Instrumentation

The instrumentation of the specimens was designed to determine the applied loads, measure deformations along the specimen, and quantify the internal stresses of the specimens. Electrical strain gages, with 6 mm gauge length, were glued to the steel tube at the midpoint of the gusset plate to measure strains at the connection zone during different stages of loading. Three strain gauges were also employed in specimens SP-H1 and SP-H2; while, two strain gauges were used for the rest of the specimens. Linear variable displacement transducers (LVDTs) were used to measure displacements at different locations of specimens as illustrated in Fig. 3. The value of the applied load was measured directly by the load cell attached to the actuator.

2.5 Loading procedure

At the beginning of the test, a small force was applied and increased gradually, meanwhile, the data acquisition system was observed to ensure that the readings are reasonable. The applied compression load was 0.5 kN/sec, which was chosen as the slowest possible loading rate in order to preclude any impact or dynamic effects and guarantee better observation of the testing procedure while preserving a reasonable testing period. Initially, the forces were increased by 2.5 kN per each successive cycle then drops to zero till reaching 25 kN. Then the load was increased accordingly with 5 kN pro each cycle until the specimens showed large deformations or failure of one of the structural elements. All the CCFT columns specimens are subjected to the same loading

Table 2 Mechanical Properties of Steel Shapes

Specimen No.	Test group	Yield stress (MPa)	Ultimate stress (MPa)	Elongation (%)	Material specification
Specimen1-Pipe	A	278.8	347.4	18.8	A53Gr-A
Specimen2-Pipe	B	293.8	356.6	30	
Specimen3-Pipe	C	267.1	347.4	33.75	
Specimen4-Pipe	D	300.6	362.7	25	
Specimen1-Plate		268.9	371.8	28	A36

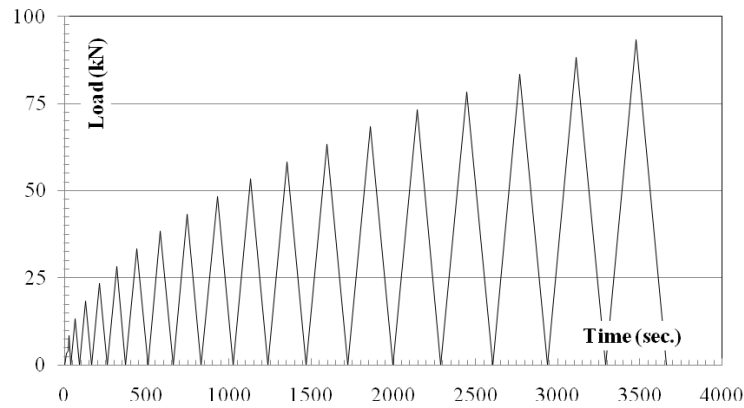


Fig. 4 Subassemblies cyclic loading pattern

Table 3 Failure modes and maximum load capacity for different specimens

Test group	Detail No.	Test uit	Max. lad (kN)	Failure mode
A	1	SP-H1	----	- Failure was not reached. - Buckling of the gusset plate was observed.
	2	SP-H2	----	- Failure was not reached. - Fracture of weld was observed.
B	1	H-1	105.0	- Bulging of the pipe shell underneath the gusset plate.
	2	H-2	103.7	- Tearing of the steel pipe. - Bulging of the pipe underneath the gusset plate.
	3	H-3	97.2	- Tearing of the steel pipe 5cm away from the gusset plate. - Bulging of the pipe underneath the gusset plate.
	4	H-4	115.8	- Bulging of the pipe shell underneath the gusset plate. - Tearing of the steel tube under the stiffeners.
	4	H-5	51.5	- large plastic deformations at the gusset plate zone.
C	1	V-1	127.7	- Bulging of the pipe shell underneath the gusset plate. - Fracture in fillet weld at the top of the gusset plate.
	2	V-2	126.0	- Tearing of the steel pipe. - Bulging of the pipe underneath the gusset plate.
	3	V-3	120.8	- Tearing of the steel pipe. - Bulging of the pipe underneath the gusset plate.
	4	V-4	114.3	- Tearing of the steel shell at the top of the gusset plate.
	4	V-5	33.6	- large plastic deformations at the gusset plate zone.
D	1	H-6	134.5	- Bulging of the pipe shell underneath the gusset plate.
	2	H-7	111.5	- Tearing of the steel pipe. - Bulging of the pipe underneath the gusset plate.
	3	H-8	200.6	- Tearing of the steel pipe 2.5cm away from the gusset plate. - Bulging of the pipe underneath the gusset plate.
	4	H-9	130.3	- Tearing of the steel pipe. - Bulging of the pipe underneath the gusset plate.
	4	H-10	56.3	- large plastic deformations at the gusset plate zone.

history which includes successive different displacement cycles according to the stepwise loading protocol as shown in Fig. 4.

3. Experimental results

The twelve specimens were tested under compressive cyclic loading till failure of the specimen or one of its elements. Specimens SP-H1 and SP-H2 of group A were not loaded till failure due to the capacity of the set-up. Table 3 summarizes the failure modes and load capacities observed for the tested subassemblies. The probable failure modes include: fracture of weld, buckling of the steel tube in compression, crushing of concrete in compression, and tearing of the steel tube in tension. The load-displacement curves, failure patterns and strain measurements of the different specimens will be discussed in the following sections.

3.1 Subassemblies load capacities and failure modes

3.1.1 Group A

Specimens of group [A] were not loaded till failure due to its higher strength and the lower capacity of the set-up. However, permanent deformations were observed in the gusset plate of test unit SP-H1. Moreover, cracks at the bottom of the fillet weld were observed in test unit SP-H2 as shown in Fig. 4. Nevertheless, the steel tube itself preserved its integrity.

3.1.2 Group B

All specimens of such group were loaded till failure. Permanent plastic deformations were observed in specimen H-1 which failed at loading level 105 kN due to bulging of the pipe shell underneath the gusset plate as shown in Fig. 6. Specimen H-2 failed at 103.7 kN due to bulging of the steel shell directly under the gusset plate and tearing of the steel pipe as shown in Fig. 7. The failure of specimen H-3 was similar H-2 except for the location of tearing and bulging of the steel tube which was 50 mm away from the end of the gusset plate and it happened at load to 97.2 kN. Specimen H4 failed at 115.8 kN due to tearing of the steel tube under the stiffeners as illustrated in Fig. 8. A significant and sudden loss of resistance was observed for the specimen H-5 at loading level 51.5 kN due to large plastic deformations at the gusset plate zone and beneath the applied load as shown in Fig. 9.

3.1.3 Group C

Specimen V-1 failed at load 127.7 kN and the observed failures were bulging of the pipe shell underneath the gusset plate and fracture in fillet weld at the top of the gusset plate as shown in Figs. 10 and 11. For specimen V-2 as shown in Figs. 12 and 13, the specimen shell was bulged underneath the gusset plate and tearing of the steel shell at the other side of the pipe was noticed at failure load 126 kN. Failure of specimen V-3 was similar V-2 except for it occurred at a lower loading level equal to 120.8 kN. The failure of test unit V-4 was due to tearing of the steel shell at the top of the gusset plate as illustrated in Fig. 14 and occurred at load 114.3 kN. A significant and sudden loss of resistance at loading level 33.6 kN was observed for the specimen V-5 due to plastic deformations at the gusset plate zone.

3.1.4 Group D

Fig. 15 shows test unit H-6 after failure. Bulging of the steel tube under the gusset plate was



Fig. 5 Fracture of weld in Test SP-H2

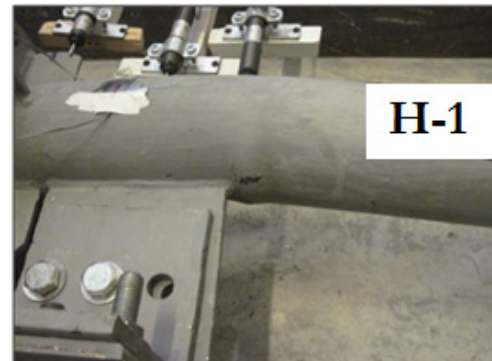


Fig. 6 Bulging of steel tube in Test H-1

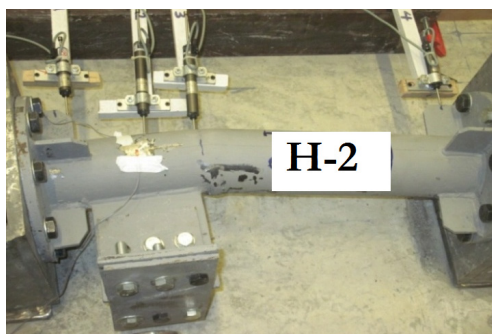


Fig. 7 Tearing of steel tube in Test H-2



Fig. 8 Tearing of steel shell in Test H-4



Fig. 9 Large plastic deformations in Test H-5



Fig. 10 Tearing of steel tube in Test V-1

observed at load 134.5 kN. The observed behavior was identical to the one observed in test unit H-1 with 28% increase in the loading capacity due to the 8% and 24% increase in the steel and concrete strength. Tearing and bulging of the steel shell directly under the gusset plate were observed at test H-7 at load 111.5 kN as shown in Figs. 16 and 17. There is an increase in loading capacity estimated by 7.5% compared to test unit H-2 due increase of steel and concrete strengths estimated by 8% and 24%, respectively. This shows that increasing the material properties affects

to some extent on the behavior of the connection. The failure of test H-8 was similar to test unit H-7 except for the failure location was 25 mm away from the end of the gusset plate as shown in Fig. 18 and the failure load was 200.6 kN. This indicates an increase in maximum loading capacity equal to about 80% compared to test unit H-3 as a result of adding another gusset plate of the same thickness. Similarly, the failure of test unit H-9 was comparable to test unit H-6 except that tearing of the steel tube was observed as illustrated in Fig. 19 and the maximum attained load was equal to

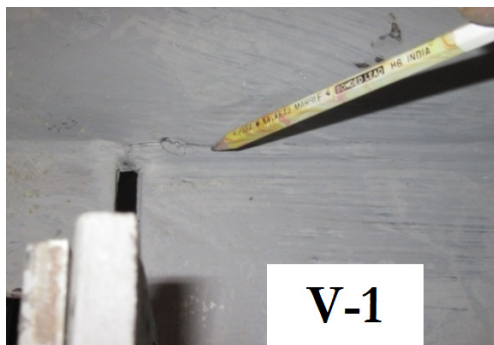


Fig. 11 Fracture of weld in Test V-1



Fig. 12 Bulging of steel tube in Test V-2



Fig. 13 Tearing of steel tube in Test V-2

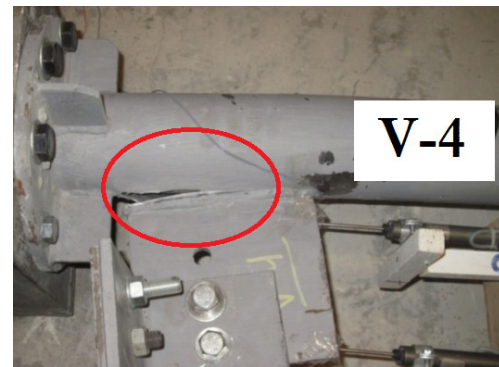


Fig. 14 Tearing of steel shell in V-4



Fig. 15 Bulging of the steel tube under the gusset plate in Test Unit H-6



Fig. 16 Tearing of the steel tube in Test Unit H-7



Fig. 17 Bulging of the steel tube under the gusset plate in Test Unit H-7

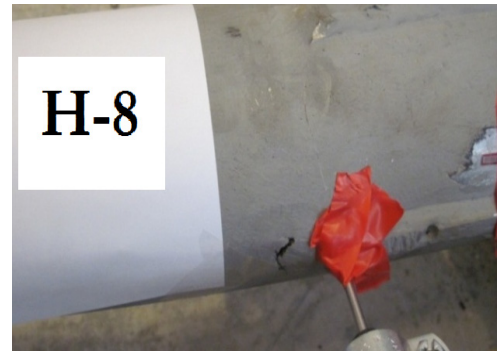


Fig. 18 Tearing of the steel tube in Test Unit H-8



Fig. 19 Tearing of the steel tube in Test Unit H-9

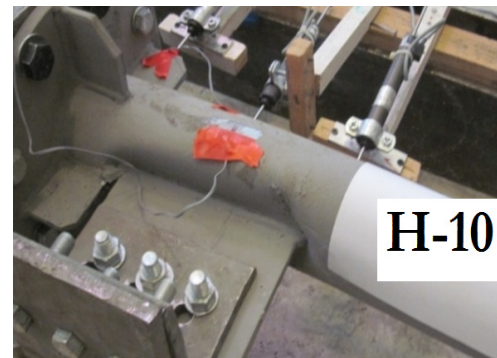


Fig. 20 Large plastic deformations in Test H-10

130.3 kN. Comparing this value to test unit H-4 shows that an increase in loading capacity equal to 13% is attained due to the 8% and 24% increase in the steel and concrete strengths. Test unit H-10 failed at loading 56.3 kN due to large plastic deformations under the applied loads as shown in Fig. 20.

3.2 Load – displacement curves

Figs. 21 through 24 show the variation of the applied load versus the displacement for the tested specimens. The displacements indicated are the values that measured only at the end of each load cycle. For the specimens loaded in the perpendicular direction, the displacements are calculated at the middle of the gusset plate, given by LVDT-2 readings, after removing the deformation resulting from the rotation of the test unit ends around the fixation point. On the other hand, the displacement for the specimens loaded in the parallel direction is calculated at the middle of the gusset plate as the average of the readings of LVDT-1 and LVDT-2. The following results can be outlined:

- The seventeen specimens showed a linear behavior followed by a nonlinear behavior developed at different loading levels according to the direction of loading and the details of the specimens as the loading increased. For test group A specimens, the nonlinear behavior

started at load 250 kN while group B specimens nonlinear behavior started at loading ranging from 60 to 80 kN. These values of loadings range changed 80 to 100 kN at group C specimens and 55 to 160 kN at group-D specimens. Specimen H-10 showed an extended linear behavior compared to the other specimens.

- The strength and capacity of the connections is enhanced with the presence of concrete-filled columns which resulted in low deterioration of the specimens. The enhancement percentages compared to hollow steel sections results reach to 55%, 74%, and 58% for test groups B, C and D, respectively. However, for group D, the percentage of enhancement for test unit H-8 was equal to 72% due to the use of a thicker gusset plate.
- Group-A specimens attained the highest load capacity due to the increased dimensions of the CFT columns and the higher concrete strength properties.
- The stiffness of groups B and D specimens was almost identical except for H-3 and H-8 with different plate thickness. The lowest stiffness is observed in tests H-1, H-4, H-6, and H-9 in which the gusset plate was directly connected to the steel tube and forces concentrate on the steel pipe shell leading to fracture failure of weld or tearing of the steel tube under the gusset plate location as observed from the failure modes.
- In group C, the load was applied to the gusset plate in the direction parallel to the CFT member which causes rotational moment at the junction between the gusset plate and the CFT column in case of connections including gusset plates welded to the steel tube. Specimens with connections details 1, 2, and 3 have the highest load capacity with an average 128 kN due to presence of gusset plate penetrating through the CFT member and the shear connectors which help to distribute the loads on the total section of the member meanwhile detail 4 has the lowest load capacity with a value 114 kN. Comparing to detail 4, the enhancement in strength for connection details 1, 2, and 3 is 11.7%, 10.2%, and 5.7%, respectively.
- In group C, the stiffness of tests V-1, V-3 and V-4 was almost identical except for V-2, which exhibits slightly higher stiffness due to the presence of the gusset plate penetrating through the connection. Higher stiffness was expected in test unit V-3; however, using gusset plate with half the thickness of the other units resulted in making its stiffness approximately equal to the other units. The stiffness of specimen V-5 was less than that

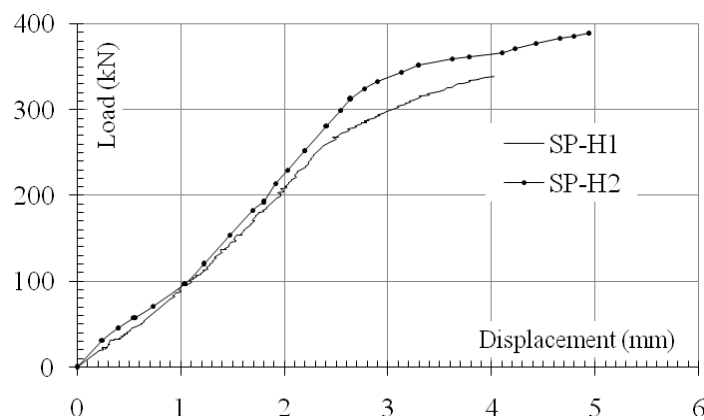


Fig. 21 Load-displacement curve of group A

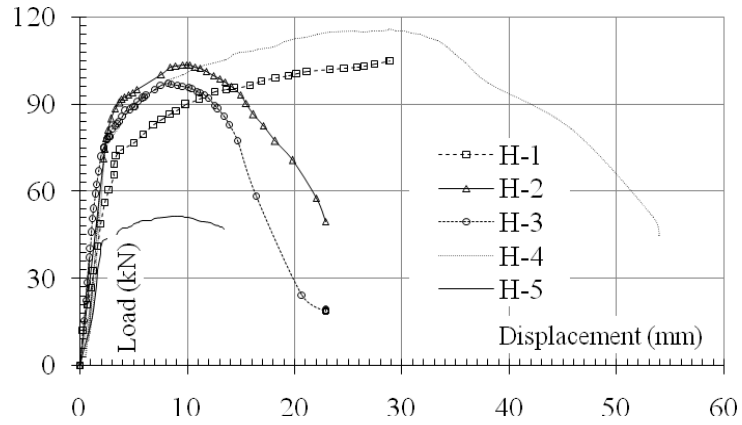


Fig. 22 Load-displacement curve of group B

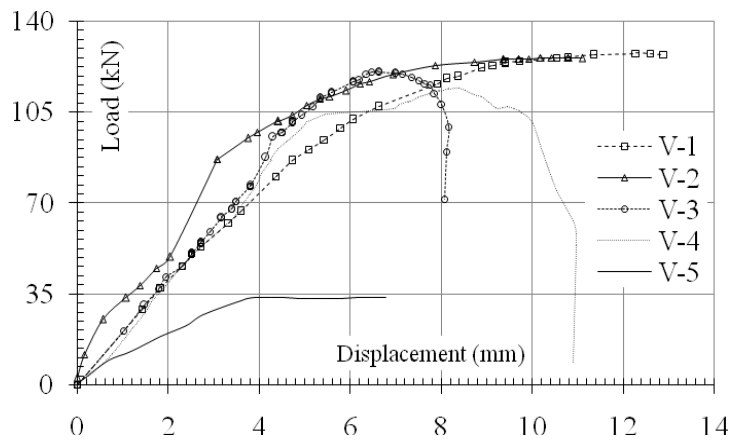


Fig. 23 Load-displacement curve of group C

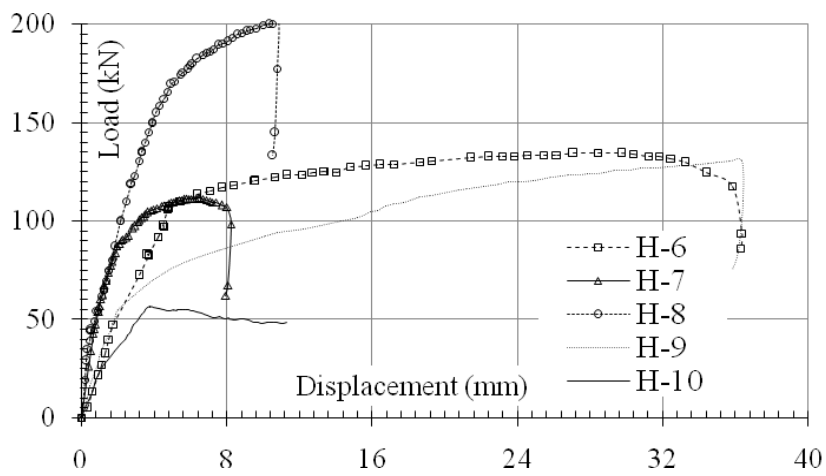


Fig. 24 Load-displacement curve of group D

exhibited by H-5 and H-10 in groups B and D, respectively due to the loading eccentricity which resulted in fast deterioration of due to stresses concentration at the end of the gusset plate and lack of the concrete infill.

- The ductility of different connections was calculated as the ratio between the displacement at failure and displacement at the end of the linear zone. For group A, the test was stopped before failure, so evaluating the ductility was not possible. For test group B, the ductility of tests H-1 and H-4 was identical since the use of shear studs did not restrain the movement under the effect of loading in the perpendicular direction. The ductility of H-3 is higher than H-2 by 14% due to the use of thinner gusset plate. The ductility of H-2 and H-3 specimens decreased by 45% compared to the ductility of H-1 and H-4 specimens due to the restraining movement under the applied loads due to presence of the gusset plate penetrating through the CFT. For test group D, the highest ductility values were observed in test units H-6 and H-9 as in group B. In addition, similar values were observed for test units H-1, H-6, H-4, and H-9 with an average difference of about 10%. Meanwhile, the least ductility value was observed in test unit H-8. A decrease in ductility equal to 62% was observed between test units with increase in load capacity equal to 35%. This behavior is expected since the increase in strength is usually accompanied by decrease in the ductility. It was also observed, by comparing test units H-3 and H-9, that doubling the thickness of the gusset plate resulted in reducing the ductility by about 90%. For test group C, the ductility of V-1 and V-2 specimens and higher than values obtained from V-3 and V-4 by 32% and 42%, respectively was almost the same. The least ductility was exhibited by test V-3.

3.3 Axial and hoop strains in pipe

The hoop strain response for test group B is illustrated in Fig. 25. Although tensile hoop strains are expected in CFT sections, tested specimens showed negative values that denote compressive stresses rather than tensile. This can be attributed to the absence of axial load on the CFT column and the direction of loading which imposes compression forces within the zone of connection. It

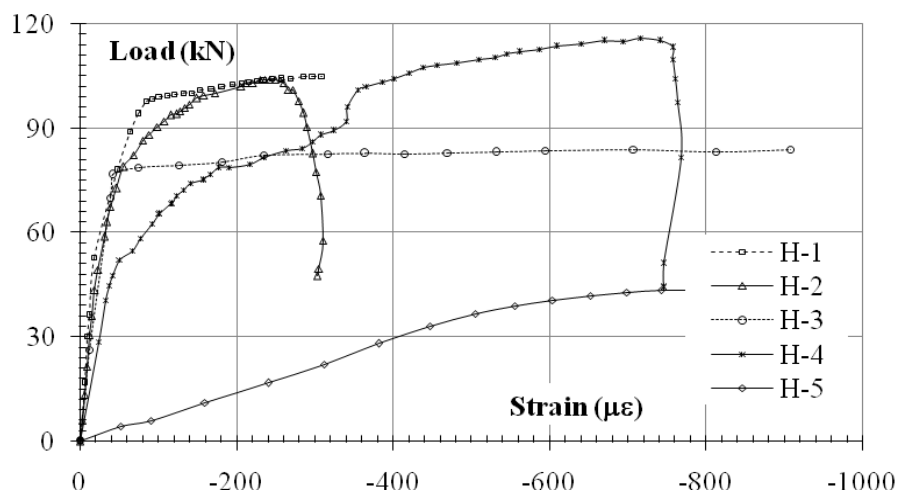


Fig. 25 Hoop strains of group B tests

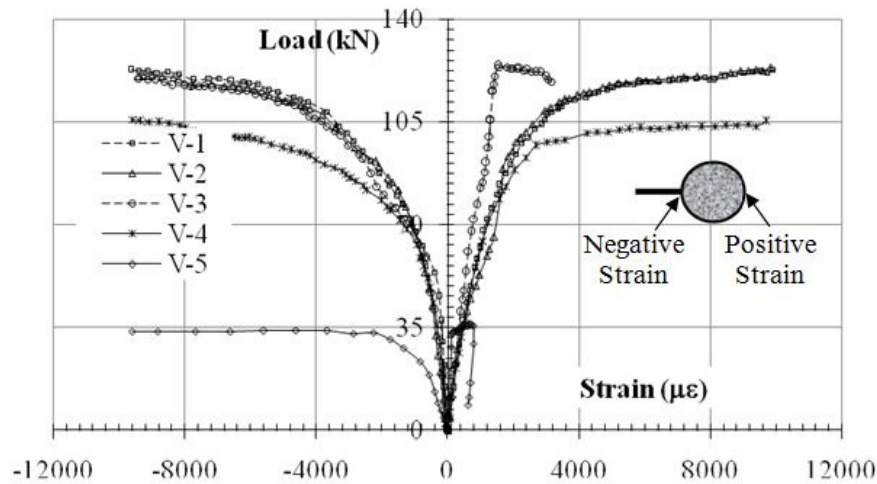


Fig. 26 Axial strains of group C tests

was observed that the bare steel column exhibited fast deterioration. The lowest hoop strain response was exhibited by test H-3 which indicates that added gusset plate is affecting the flow of stresses. Fig. 26 shows the axial strains measured at both sides of specimens for test group C. The neutral axis of the section was almost at the center for tests V-1, V-2, and V-4. It was observed that the strain response for test V-4 is lower than the other units which explain the lower load capacity carried by this joint compared to the other joints. For test V-3, the positive and negative strain responses were not identical which indicated that adding gusset plate in the connection changed the distribution of stresses on section. For test V-5, the compressive strains were larger than the corresponding tensile ones due to deformation of the pipe under the gusset plate.

4. Conclusions

This paper presented the experimental results of a series of gusset plate to CCFT connections with different configurations. The tested subassemblies consisted of a part of a circular CFT (CCFT) column with the studied connection welded at its end. The experiments showed variability in behavior of connections depending on its configuration and loading direction. The main conclusions drawn from the tests are summarized below:

- Local bulging of steel shell under the gusset plate was found to be a dominant failure mode for connections where the gusset plate is directly welded to the steel tube. Meanwhile, tearing of the steel tube at the tension side was the main failure mode for connections with gusset plate penetrating through the CFT column.
- For connections with strength lower than the adjacent members, brittle failure modes are most likely to occur.
- When a composite column is used, the strength and stiffness is substantially increased as compared to the bar steel column. In the bare steel one, failure was caused by large plastic deformations of the column wall. It was found that the addition of concrete infill increased

the capacity of the joints by 55% and 74% for connections loaded parallel and perpendicular to the specimen axis, respectively.

- CCFT connections the subjected to perpendicular compression to the column axis, exhibited higher values of load capacity for test units with gusset plate welded directly to the steel tube. Meanwhile, the lowest load capacity was observed in the test unit imposing higher loads on the steel thin shell. On the other hand, the capacity of the connections subjected to shear loading which is parallel to the specimen axis, showed higher values for test units with gusset plate penetrating through the steel tube. This shows that the behavior of connections depends to some extent on the inclination of the brace force.
- The stiffness of connections is almost identical when loaded with compression; however, connections with gusset plate penetrating through the CFT column showed higher stiffness values when they are shear loaded.
- As design point of view, CCFT connections with extended gusset plates penetrating the column tubes are preferable since they exhibit higher capacity and ductility when subjected to shear loadings. Meanwhile, when the connections are subjected to axial compression loading, presence of gusset plates inside the columns increase the capacity and reduce the ductility.

Acknowledgments

This research was funded by the Civil Engineering Research Center, Faculty of Engineering, Cairo University. The experimental testing was performed at the Construction Engineering Laboratory, the American University in Cairo. The cooperation and assistance of the technical staff of the laboratory is gratefully acknowledged.

References

- AISC (2010), Draft Specification for Structural Steel Buildings, ANSI/AISC 360-10, American Institute of Steel Construction, Inc., Chicago, IL, USA, August.
- Denavit, M.D. and Hajjar, J.F. (2012), "Nonlinear seismic analysis of circular concrete-filled steel tube members and frames", *J. Struct. Eng., ASCE*, **138**(9), 1089-1098.
- Gross, J.L. (1990), "Experimental study of gusseted connections", *Eng. J., AISC*, **27**(3), 89-97.
- Hajjar, J.F., Denavit, M.D., Perea, T. and Leon, R.T. (2012), "Seismic design and stability assessment of composite framing systems", *Proceedings of 2012 Urban Earthquake Engineering*, Tokyo, Japan, March.
- Hassan, M.M., Ramadan, H.M., Abdel-Mooty, M. and Mourad, S.A. (2013), "Cyclic behavior of beam-bracing-CFT column connections in concentrically braced frames", Doctor of Philosophy Thesis, Cairo University, Faculty of Engineering, Cairo, Egypt.
- Hassan, M.M., Ramadan, H.M., Abdel-Mooty, M. and Mourad, S.A. (2013), "Behavior of concentrically loaded CFT braces connections", *J. Adv. Res.*, Cairo University, **5**, 243-252.
- Hu, T., Chen, W. and Huang, Y. (2011), "Nonlinear finite element analysis of CFT-to-bracing connections subjected to axial compressive forces", *Eng. Struct.*, **33**(5), 1479-1490.
- Jacobs, W.P. and Hajjar, J.F. (2010), "Load transfer in composite construction", *Proceedings of 2010 ASCE/SEI Structures Congress*, Orlando, FL, USA, May.
- Leon, R.T. Kim, D.K. and Hajjar, J.F. (2007), "Limit state response of composite columns and beam-columns", *Eng. J., AISC*, **44**(4), 341-358.
- MacRae, G.A., Roeder, C.W., Gunderson, C.A. and Kimura, Y. (2004), "Brace-beam-column connections

- for concentrically braced frames with concrete filled tube columns”, *J. Struct. Eng., ASCE*, **130**(2), 233-243.
- Roeder, C.W., MacRae, G.A., Gunderson, C.A. and Lehman, D.E. (2003), “Seismic design criteria for CFT braced frame connections”, *Proceedings of 2003 International Workshop on Steel and Concrete Composite Construction*, Taipei, Taiwan, October.
- Roeder, C.W., Lehman, D.E. and Yoo, J.H. (2004), “Performance-based seismic design of braced-frame gusset plate connections”, *ECCS/AISC Workshop: Connections in Steel Structures*, pp. 167-176.
- Tsai, K.C. and Hsiao, P.C. (2008), “Seismic performance of buckling-restrained braces and connections”, *Earthq. Eng. Struct. D.*, **37**(7), 1099-1115.
- Whitmore, R.E. (1952), “Experimental investigation of stresses in gusset plates”, Bulletin No. 16, Engineering Experiment Station, University of Tennessee, Knoxville, TN, USA.
- Yam, M.C.H. and Cheng, J.J.R. (2002), “Behavior and design of gusset plate connections in compression”, *J. Const. Steel Res.*, **58**(5-8), 1143-1159.
- Zhang, J., Mark, D.D., Hajjar, J.F. and Lu, X. (2012), “Bond behavior of concrete-filled steel tube (CFT) structures”, *Eng. J., AISC*, **49**(4), 169-185.

CC